

# Matching hand radiographs

J.A. Kauffman<sup>1</sup>, C.H. Slump<sup>1</sup>, H.J. Bernelot Moens<sup>2</sup>

<sup>1</sup>University of Twente, P.O.Box 217, 7500 AE Enschede, The Netherlands

E-mail: [j.a.kauffman@ewi.utwente.nl](mailto:j.a.kauffman@ewi.utwente.nl)

<sup>2</sup>Hospital Group Twente, Hengelo, The Netherlands

*Abstract*— **Biometric verification and identification methods of medical images can be used to find possible inconsistencies in patient records. Such methods may also be useful for forensic research. In this work we present a method for identifying patients by their hand radiographs.**

We use active appearance model representations presented before [1] to extract 64 shape features per bone from the metacarpals, the proximal, and the middle phalanges. The number of features was reduced to 20 by applying principal component analysis. Subsequently, a likelihood ratio classifier [2] determines whether an image potentially belongs to another patient in the data set.

Firstly, to study the symmetry between both hands, we use a likelihood-ratio classifier to match 45 left hand images to a database of 44 (matching) right hand images and vice versa. We found an average equal error probability of 6.4%, which indicates that both hand shapes are highly symmetrical. Therefore, to increase the number of samples per patient, the distinction between left and right hands was omitted.

Secondly, we did multiple experiments with randomly selected training images from 24 patients. For several patients there were multiple image pairs available. Test sets were created by using the images of three different patients and 10 other images from patients that were in the training set. We estimated the equal error rate at 0.05%.

Our experiments suggest that the shapes of the hand bones contain biometric information that can be used to identify persons.

*Keywords*— **hand radiographs, model, biometric verification, identification**

## I. INTRODUCTION

It is likely that large databases of patient records that are used in clinical trials contain a significant number of false entries and other inconsistencies. In the process of data acquisition, data analysis and administration there are several stages where patient data can be filed incorrectly. Particularly when information is passed through with paper forms (illegible handwriting) or

manual entry, there is a high risk for errors, such as the misspelling of names, mixed up records, and wrong numbers. As a result these errors may compromise the outcome of a medical trial.

There are several statistical methods to search through databases for unusual deviations in numbers, but this is less straightforward for other information in patient records, such as radiographs. In our case, we are interested in verifying databases of hand radiographs. Our goal is to identify possible errors, such as double entries (one patient filed under more than one name), wrong patient labels (different patients filed under the same name), and mirrored images (left and right mixed up). To accomplish this, we look for characteristic features in the shapes of the hand bones. Next we use a classification method to compare these ‘biometric features’ of the images in our dataset. Then we determine for each image how likely it is that it is filed correctly.

Using the shape of hands for biometric verification and identification is not new. Similar methods exist for using the outer geometry of the hand [3;4]. In [5] it is suggested that hand radiographs can be used for this purpose, but thus far we are not aware of any other research on this subject.

Besides detecting patient database inconsistencies and preventing faulty entries, biometric identification of bones may be useful for forensic applications. Other applications may be found in the security field. Though X-rays are seldom used for this purpose, sometimes low dose X-ray scanners are used for searching people for weapons and contrabands. A biometric identification system could be a valuable extension to such systems.

## II. METHODS

### A. Data

In our experiments we have used a set of 89 posterior anterior single hand radiographs (45 left and 44 right hands) of 27 patients. The number of radiographs per

patient varied between one and four image pairs (Figure 1). For one patient there was an extra radiograph of the left hand.

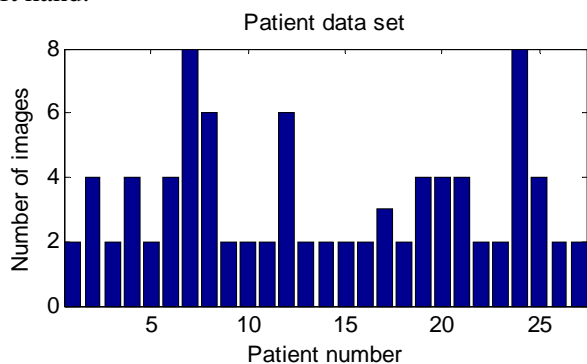


**Figure 1: Histogram displaying the number of available images for each patient in the dataset.**

### B. Biometric features

The contours of the bones are used as biometric features for our classification algorithm. The contours are described with 64 points per bone. The bones used for our feature description are the metacarpals, the proximal and middle phalanges (Figure 2). These are 14 bones in total.

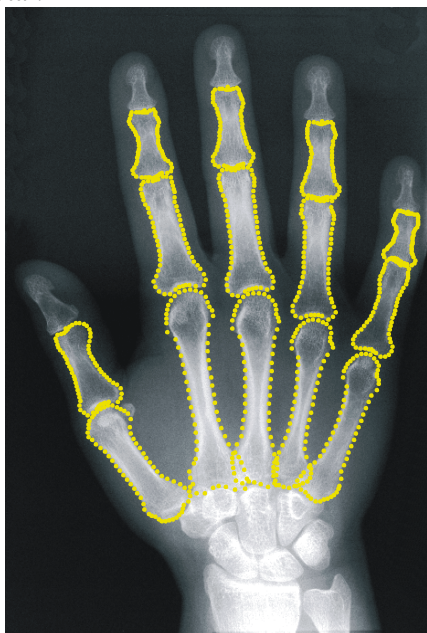


**Figure 2: The contours of 14 bones are used for feature extraction.**

The contour points can be extracted manually or automatically with the active appearance model search algorithm described in [1]. Each bone shape is described with 64 points according to the crossings of a fishbone shaped grid with the bone contour (Figure 3).

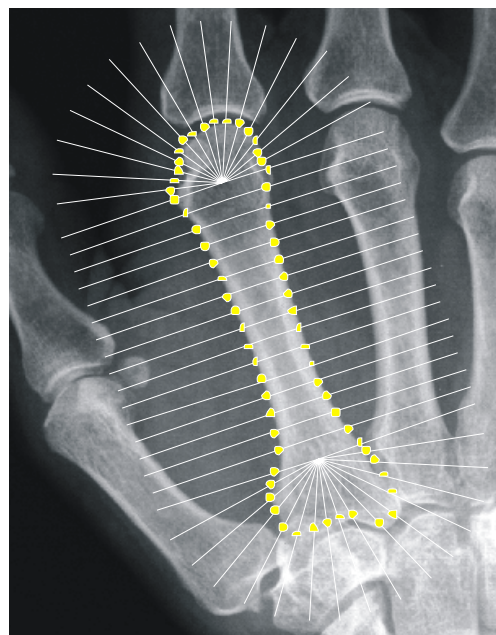


**Figure 3: For each bone 64 landmarks are defined by determining the crossings of a fishbone shaped grid and the bone contour.**

Though most image pairs had been labeled ‘left’ or ‘right’, we treated both the same by mirroring all left hand images. This also makes it easier to compare both hands with each other.

As the positioning of the fingers may vary between radiographs, we need to compensate for this variability. Figure 4 shows the major positioning variability due to lateral flexion of the joints. Notice that the phalanges of a finger cannot be flexed laterally, and that therefore any angle between them is a characteristic feature. By ‘dissecting’ the moveable parts we obtain 7 new parts of single bones or connected bone groups (Figure 5). Next we center these parts to the origin of the coordinate system and rotate them to a uniform position. The bones are rotated such that the selected axes of the bones become vertically aligned. This alignment makes the bone shapes invariant to positioning, while keeping information about the ‘straightness’ of the fingers and the internal locations of the metacarpals.

The features that are extracted from these bone groups are the  $x$ - $y$  coordinates of the contour points in their aligned coordinate frame. This results in a feature vector  $\mathbf{x}$  of 1792 ( $14 \times 64 \times 2$ ) elements for each hand in the dataset.

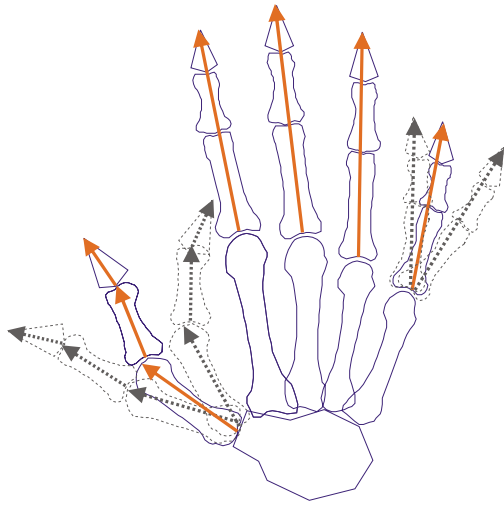


**Figure 4: Variability in finger positioning due to lateral flexion of joints. The arrows indicate which parts can be moved.**

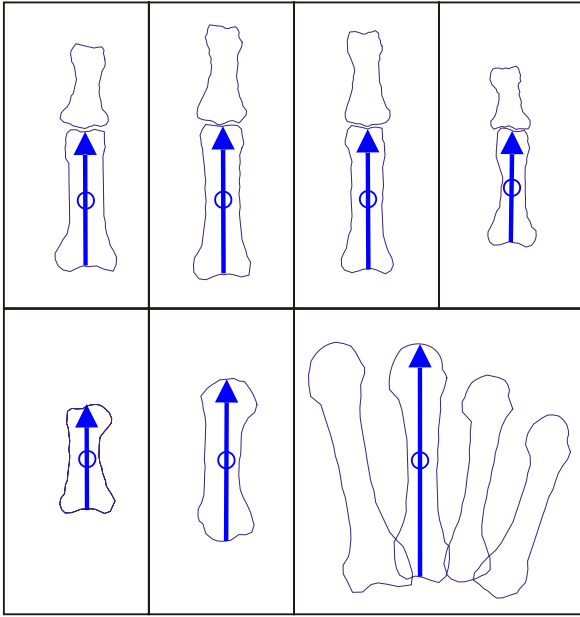


**Figure 5: The selected landmarks of each moveable part is centered and rotated to a uniform position. The arrows show which axes are selected for the alignment of the bones. The circles indicate the origins.**

### C. Classification

The bone shapes are matched with a Likelihood-ratio classifier for Gaussian probability densities [2]. We consider that a set of features in a patient's record indeed originate from the pertinent patient or from another patient which may or may not be present in the dataset. The features of the pertinent patient is characterized by a mean  $\mu_w$  and a 'within-class' covariance matrix  $\Sigma_w$  and the features of the total dataset is characterized by  $\mu_T$

and  $\Sigma_T$ . Then a similarity score  $S(x)$  can be derived from the log-likelihood ratio:

$$S(x) = -(x - \mu_w)^T \Sigma_w^{-1} (x - \mu_w) + \dots - (x - \mu_T)^T \Sigma_T^{-1} (x - \mu_T) \quad 1$$

Since the covariance matrices are unknown, these have to be determined from a training set. For an accurate estimation this would require many more training examples than we have in our image set. Therefore we reduce the number of features by applying a principal component analysis (PCA) on all samples of the training set [6]. To do this we create a matrix  $X$  which columns are  $N_s$  sample feature vectors with the overall mean subtracted.

$$X = [x_1 - \mu_T, \dots, x_{N_s} - \mu_T] \quad 2$$

A singular value decomposition (SVD) of the matrix  $X$  is used to find the  $N_s \times N_s$  orthonormal matrices  $U_X$  and  $V_X$ , and a non-negative diagonal matrix of singular values  $S_X$ .

$$X = U_X S_X V_X^T \quad 3$$

The number of dimensions in the data is reduced by taking submatrix  $V_{PCA}$ , containing the first  $N_{PCA}$  principal columns of  $V_X$ , and the first  $N_{PCA} \times N_{PCA}$  submatrix of  $S_X$ ;  $S_{PCA}$ . The data with reduced dimensions is then:

$$Y = S_{PCA} V_{PCA}^T \quad 4$$

The number of dimensions  $N_{PCA}$  is chosen such that the variance displayed in the training set is covered for 95% (in our experiments  $N_{PCA}=25$ ).

Since we do not have sufficient data of every patient to calculate the covariance matrix per patient, we estimate the within-class variance. Therefore we create a matrix  $W$  which contains the feature vectors from  $Y$  with the subtracted means of the corresponding users:

$$W = [Y_1 - \mu_1, \dots, Y_{N_{user}} - \mu_{N_{user}}] \quad 5$$

An SVD is used to calculate the  $N_{PCA} \times N_{PCA}$  orthogonal matrices  $U_W$  and  $V_W$ , and a non-negative diagonal matrix of singular values  $S_W$ :

$$W = U_W S_W V_W^T \quad 6$$

Next, we normalize the column vectors in  $U_W$  with  $S_W$  to

$$U_{Wnorm} = \sqrt{N_s - 1} U_W S_W^{-1} \quad 7$$

From this matrix we create a submatrix  $U_{LDA}$  by taking the principal  $N_{LDA}$  column vectors (for our experiments  $N_{LDA}=20$ ). Next we use this matrix to do a dimension

reduction on our data by means of linear discriminant analysis (LDA) [7]. The new data then becomes:

$$\mathbf{Z} = \mathbf{U}_{\text{LDA}}^T \mathbf{Y} \quad 8$$

Another SVD is used to calculate the covariance matrix of  $\mathbf{Z}$  and the orthogonal transformation matrix  $\mathbf{U}_Z$ .

$$\mathbf{Z} = \mathbf{U}_Z \mathbf{S}_Z \mathbf{V}_Z^T \quad 9$$

The covariance matrix then becomes:

$$\Sigma_Z = \frac{1}{N_s - 1} \mathbf{S}_Z^2 \quad 10$$

The described sequence of transformations can be combined in

$$\mathbf{T} = \mathbf{U}_Z^T \mathbf{U}_{\text{wnorm}}^T \mathbf{U}_X^T \quad 11$$

Now let  $\mathbf{u}$  and  $\mathbf{v}_i$  be the transformed input-vector with subtracted means  $\mu_T$  and  $\mu_i$ :

$$\mathbf{u} = \mathbf{T}(\mathbf{x} - \mu_T), \quad 12$$

$$\mathbf{v}_i = \mathbf{T}(\mathbf{x} - \mu_i),$$

where  $\mu_i$  is the mean feature vector of a patient to be matched and  $\mu_T$  the mean of the total dataset. Then the similarity score can be calculated by

$$S_i(\mathbf{u}, \mathbf{v}) = -\mathbf{v}_i^T \mathbf{v}_i + \mathbf{u}^T \Sigma_Z^{-1} \mathbf{u} \quad 12$$

A predetermined threshold decides whether the image belongs to the pertinent patient or to another.

### III. RESULTS

#### A. Matching left and right hands

Tests have been done on the dataset described under Methods. In the first experiment we have tested if it would be possible to identify patients by their left hand using the features of their right hand. To investigate this, we used all 44 right hand images as the training set for determining the within class variability and the individual patient templates. The remaining 44 left hand images were used as the test set.

Figure 6 shows the false-positive rate (FPR) and the false-negative rate (FNR) versus the output score of the classifier and Figure 7 shows the receiver-operating characteristics (ROC) curve. The equal error rate is at 6.1%.

Similar results were obtained by using the left hand images in the training set and the right in the test set. The resulting equal error rate was 6.7%

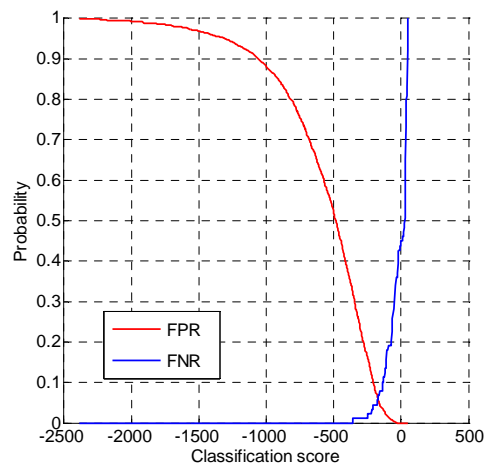


Figure 6: FPR and FNR versus the classification score. The equal error rate is at 6.1%.

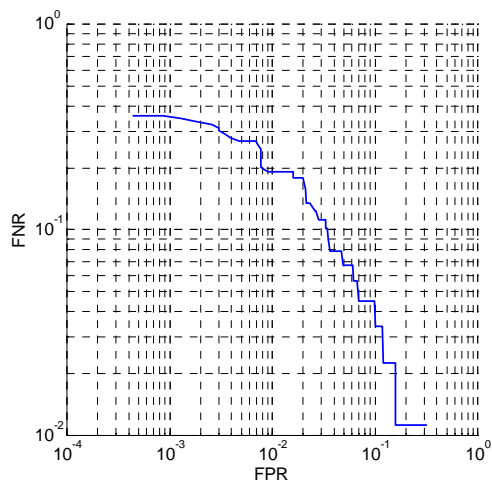
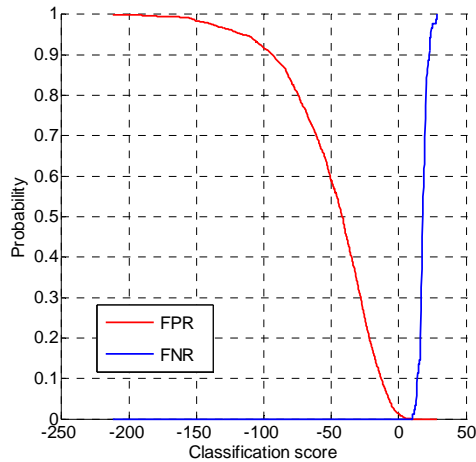


Figure 7: ROC curve of the FNR versus the FPR.

#### B. Testing the dataset for errors

To test our dataset for any possible errors, we have matched each image of the dataset to the features of all patients. As a result of this experiment we found that the images of one patient matched to the features of another. After an inquiry in the originating hospital's records, we found that these radiographs had been filed incorrectly.

After correction of this error, we performed multiple tests on the data set. For each test we used the images of 24 randomly selected patients in the training set. The images of the remaining patients were included into the test set, together with 10 images from patients that were in the test set. The results of the similarity scores are displayed as false-positive rates and false-negative rates in Figure 8. The estimated equal error rate is at 0.05%.



**Figure 8: FPR and FNR versus the classification score. The equal error rate is at 0%.**

#### IV. CONCLUSION

We have demonstrated a method to extract biometric features from the shapes of the hand bones, being invariant to the positioning of the hand and fingers. These features can be used to verify a patient's identity and to detect possible inconsistencies in a patient database. As a proof of concept, we found an unforeseen error in our dataset. Also we found that the human hands are sufficiently symmetric to match one hand with the other.

#### REFERENCES

- [1] Kauffman, J. A., Slump, C. H., and Bernelot Moens, H. J. Segmentation of hand radiographs with multilevel connected active appearance models. *Medical Imaging 2005: Image Processing* 5747-182. 2005. SPIE.
- [2] Bazen, A. M. and Veldhuis, N. J., "Likelihood-ratio-based biometric verification," *IEEE Transactions on Circuits and Systems for Video Technology*, vol. 14, no. 1, pp. 86-94, Jan.2004.
- [3] Jain, A. K., Ross, A., and Pankanti, S. A prototype hand geometry-based verification system. *Proceedings of the second International Conference on Audio- and Video-Based Personal Authentication (AVBPA)*, 166-171. 3-22-1999. Washington.
- [4] Veldhuis, R. N. J., Bazen, A. M., Booij, W., and Hendrikse, A. A comparison of hand-geometry recognition methods based on low- and high-level features. *ProRISC workshop 2004*. 2004.
- [5] Thodberg, H. H. Hands-on Experience with Active Appearance Models. *Sonka and Fitzpatrick. Medical Imaging 2002: Image Proceedings* 4684, 495-506. 2002. SPIE.
- [6] Gerbrands, J. J., "On the relationships between SVD, KLT and PCA," *Pattern Recognition*, vol. 14, no. 1-6, pp. 375-381, 1981.
- [7] Trees, H. V., *Detection, estimation, and modulation theory* New York: Wiley, 1968.